

SERIAL PROCESSING AFTER LUNAR ANORTHOSITIC CRUST FORMATION INDICATED BY RARE EARTH ELEMENTS IN PLAGIOCLASE

D. Ji, N. Dygert, Department of Earth and Planetary Sciences, University of Tennessee, Knoxville, TN, 37916, (dji2@vols.utk.edu).

Introduction: The classical lunar magma ocean (LMO) hypothesis argues that the lunar anorthosites form from floating LMO crystallized plagioclase [e.g., 1]. To evaluate the formation of the lunar anorthosites in the context of the magma ocean hypothesis, we modeled their Eu and REE contents using experimentally determined LMO solidification sequences [e.g. 2-4] assuming different major and trace element compositions for the LMO, using temperature (T), pressure, composition, and oxygen fugacity (fO_2)-dependent partition coefficient models [e.g. 5-7]. Compared to natural plagioclase with variable Eu anomalies (Eu/Eu^* of 5-122) and REE slopes, the calculated plagioclase crystallized by the LMO have larger positive Eu anomalies (~ 100 -1000) and constant REE slopes under lunar-relevant fO_2 s (Fig. 1). We conclude that the Eu anomaly and REE pattern exhibited by lunar plagioclase cannot be explained by LMO solidification alone.

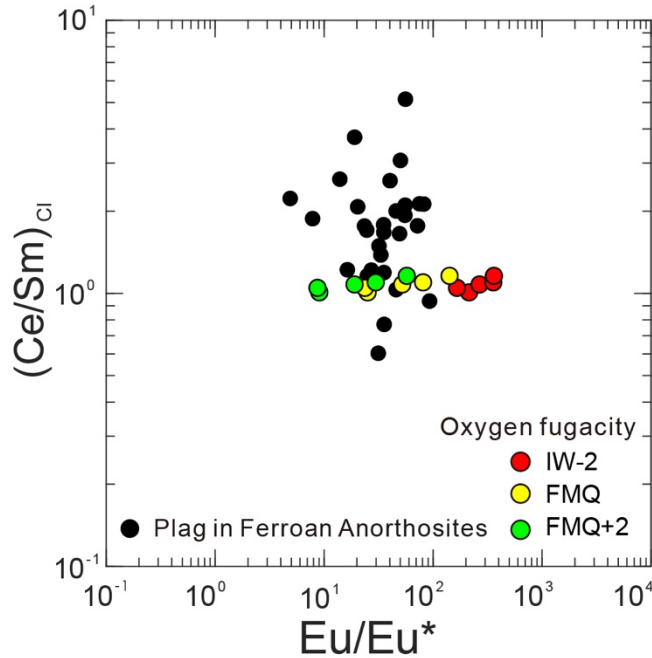


Fig. 1. Modeled plagioclase formed by LMO crystallization (colored circles) under different percent solidification and fO_2 conditions compared to plagioclase in returned ferroan anorthosites [8] (black circles). The chondrite-normalized Ce/Sm ratio is shown on the y-axis and Eu/Eu^* is shown on the x-axis. These simulations show representative results based on the solidification sequence from [2]. The trace element composition of the bulk LMO assumed is depleted MORB mantle [9]. Simulation results assuming different solidification sequences and initial trace element compositions are similar. The models show that most of the lunar anorthosites cannot be modeled as direct solidification products of a lunar magma ocean, particularly for low lunar-relevant fO_2 s.

Subsolidus reequilibration subsequent to magma ocean solidification successfully models the anorthosites: We explored a series of possible mechanisms that could reconcile plagioclase from the LMO with the lunar ferroan anorthosites, including (a) partial melting of the anorthosites, (b) closed-

system fO_2 and T -dependent subsolidus reequilibration, (c) subsolidus reequilibration after addition of a chondritic component, and (d) subsolidus reequilibration after addition of an interstitial trapped LMO liquid, all of which failed to model the distribution of natural samples. Finally, we explored subsolidus reequilibration after addition of a minor KREEP component (data from [10]). Subsolidus reequilibration under variable fO_2 and T conditions changes the Eu anomaly magnitude as well as the slope of REE patterns, while the addition of minor KREEP reduces Eu anomalies and elevates Ce/Sm ratios. The more KREEP is added, the more the Eu anomaly decreases and the greater the slope of REE patterns (Fig. 2). Different combinations of T , fO_2 and KREEP reproduce variations among the natural samples.

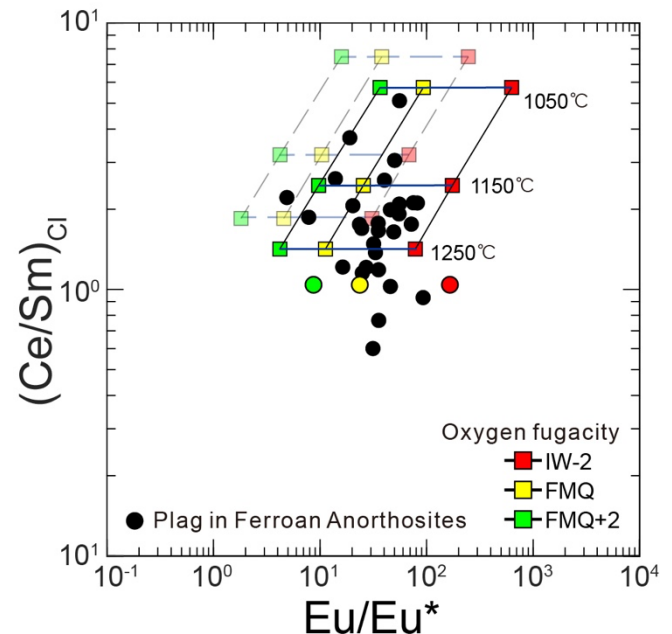


Fig. 2. Modeled plagioclase after subsolidus reequilibration under different T and fO_2 conditions after the addition of KREEP component. Black circles show lunar plagioclase in returned ferroan anorthosites [8]. Y-axis is chondrite-normalized Ce/Sm, X-axis is Eu/Eu^* . Simulations assuming addition of 0.1% KREEP are shown by opaque symbols and solid lines, and simulations assuming addition of 0.5% KREEP are shown by the partially transparent symbols and dashed lines. In the simulations shown here, we assume the mineral mode of anorthosite is 95.1 % plagioclase + 4.9 % low-Ca pyroxene. Because plagioclase crystallizes in multiple stages in the LMO solidification sequence, the plagioclase here are those crystallized from one specific part of the solidification sequence (82 percent solidification). Other modeling conditions are the same as described in Fig. 1.

Monte Carlo simulations constrain lunar properties and conditions of subsolidus reequilibration: We further evaluated the lunar fO_2 , percent solidification (PCS) that anorthosites crystallized from the LMO, the T of subsolidus reequilibration, and the proportion of KREEP component added to the anorthosites by Monte-Carlo simulations. The

results show that anorthosite crystallized from relatively late stages of LMO solidification, and reequilibration occurs at 1100-1200 °C after the addition of less than 1% of a KREEP component (Fig. 3). The above conditions are consistent for all assumed initial bulk LMO compositions and crystallization sequences. We additionally investigated another end-member possibility, that all mafic minerals crystallized by interstitial trapped liquid between plagioclase, and the results maintain great similarity.

Among several different initial bulk Moon trace element compositions we evaluated, light-REE (LREE) depleted compositions (i.e., depleted MORB mantle (DMM) [8], and diluted N-MORB [11]) produce the largest number of successful simulations, reproducing almost every natural sample. Simulations testing a chondritic bulk LMO produce fewer successful simulations, especially for LREE depleted natural samples. Diluted N-MORB and DMM show similar REE patterns, i.e., relative depletion in LREE compared to heavy-REEs (HREEs). An initial bulk LMO with LREE depletion better fits the natural plagioclase with lower (Ce/Sm)_{Cl}, while addition of LREE enriched KREEP increases the (Ce/Sm)_{Cl} in plagioclase after subsolidus reequilibration, successfully modeling samples with LREE enrichment. The most successful simulations invoked a bulk LMO with a DMM trace element composition, implying that the initial bulk Moon may be LREE-depleted, as previously suggested by isotopic investigations of ferroan anorthosites [e.g., 12].

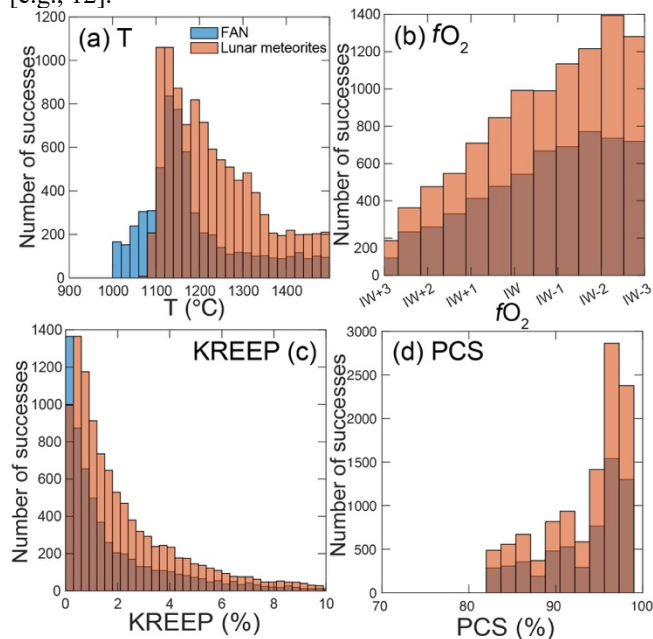


Fig. 3. Monte-Carlo simulations testing conditions under which subsolidus reequilibration after minor KREEP addition reproduce the compositions of lunar FANs and meteorites. The assumed mineral mode of lunar anorthosite is the average of 15 Apollo FANs we compiled (95.5% plag + 3.4% low-Ca px + 1.1% high-Ca px). The model assumes partition coefficients calculated using major elements averaged from measured plagioclase and pyroxene for both FAN [8] and lunar meteorites [e.g., 13, 14]. The modeled plagioclase crystallized from 82 to 98 percent solidification of the LMO; other modeling conditions are the same as described in Fig. 1. The threshold to filter successful simulations is 20 % variation from observed Eu/Eu* and Ce/Sm in the lunar plagioclase. Most of

the successfully simulated T_s are around 1100-1200 °C, fO_{2s} are around IW-2, the percentage of KREEP added is less than 1%, and crystallization of anorthosite happened at a relatively late stage of LMO solidification (PCS).

Serial processing after a cumulate mantle overturn event:

The addition of a KREEP component suggests secondary processing of the lunar plagioclase. Based on the simulation results, we propose a post-LMO serial processing model to explain the petrogenesis of lunar anorthositic crust (Fig. 4), which differs from traditional serial magmatism models [e.g., 15] because it invokes modification of a relatively pure anorthositic proto-crust that formed in the LMO. After LMO solidification, cumulate mantle overturn [e.g., 16] is thought to produce upwelling of hot materials from the interior of the Moon, which would melt. These melts may intrude into the crust, becoming the parental magmas of Mg-suite. They and their overturned sources would heat the lower anorthositic crust (crystallized in late stages of LMO solidification), forming low-density anorthitic diapirs which buoyantly migrated into the upper crust. These diapirs (contaminated by KREEPy liquid before and/or during upwelling) would undergo subsolidus reequilibration, producing plagioclase in lunar anorthosite with Eu anomalies and REE patterns consistent with natural samples (Fig. 2). This serial processing model is supported by the overlap of ages between ferroan anorthosites and Mg-suite [e.g. 17].

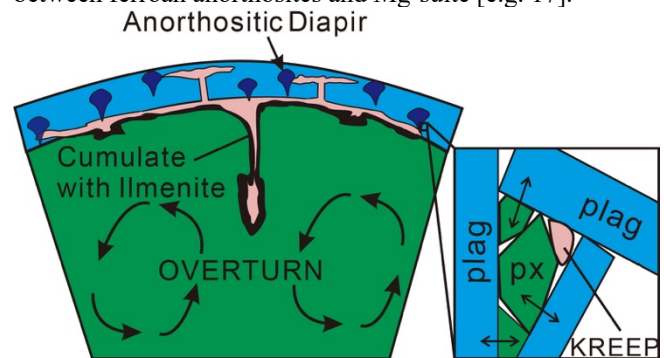


Fig. 4. Cartoon illustrating serial processing of the lunar crust after magma ocean solidification. During the cumulate mantle overturn event, hot material from the lunar interior upwells to the base of the crust, heating anorthosites hybridized by KREEPy liquid at the bottom of the crust. Anorthositic diapirs move toward the crustal surface during and/or after subsolidus reequilibration.

References: [1] Warren (1985) *AREPS* **13**, 201-240. [2] Charlier et al. (2018) *GCA* **234**, 50-69. [3] Lin et al. (2017) *EPSL* **471**, 104-116. [4] Rapp & Draper (2018) *MAPS* **53**, 1452-1455. [5] Sun et al. (2017) *GCA* **206**, 273-295. [6] Dygert et al. (2014) *GCA* **132**, 170-186. [7] Dygert et al. (2020) *GCA* **279**, 258-280. [8] Pernet-Fisher et al. (2019) *GCA* **266**, 109-130. [9] Workman & Hart (2005) *EPSL* **231**, 53-72. [10] Warren & Wasson (1979) *RG* **17**, 73-88. [11] Arevalo & McDonough (2010) *CG* **271**, 70-85. [12] Boyet et al. (2015) *GCA* **148**, 203-218. [13] Cahill et al. (2004) *MAPS* **39**, 503-529. [14] Roberts et al. (2019) *MAPS* **54**, 3018-3035. [15] Longhi (2003) *JGR: Planets* **108**, E8. [16] Hess & Parmentier (1995) *EPSL* **134**, 501-514. [17] Dygert et al. (2017) *GRL* **44**, 11-282.